

Stable top-up operation at SPring-8

Hitoshi Tanaka,^{a,b*} Masatoshi Adachi,^c Tsuyoshi Aoki,^a Takao Asaka,^a Alfred Baron,^a Shin Daté,^a Kenji Fukami,^a Yukito Furukawa,^a Hirofumi Hanaki,^a Naoyasu Hosoda,^a Tetsuya Ishikawa,^{a,d} Hiroaki Kimura,^a Kazuo Kobayashi,^c Toshiaki Kobayashi,^a Shinji Kohara,^{a,b} Noritaka Kumagai,^a Mitsuhiro Masaki,^a Takemasa Masuda,^a Sakuo Matsui,^a Akihiko Mizuno,^a Takeshi Nakamura,^a Takeshi Nakatani,^e Takashi Noda,^a Toru Ohata,^a Haruo Ohkuma,^a Takashi Ohshima,^{a,b} Masaya Oishi,^a Sigeki Sasaki,^a Jun Schimizu,^a Masazumi Shoji,^a Kouichi Soutome,^a Motohiro Suzuki,^a Shinsuke Suzuki,^a Yoshio Suzuki,^a Shirou Takano,^a Masaru Takao,^a Takeo Takashima,^a Hideki Takebe,^a Akihisa Takeuchi,^a Kazuhiro Tamura,^a Ryotaro Tanaka,^a Yoshihito Tanaka,^{d,b} Tsutomu Taniuchi,^a Yukiko Taniuchi,^a Kouji Tsumaki,^a Akihiro Yamashita,^a Kenichi Yanagida,^a Yoshitaka Yoda,^a Hiroto Yonehara,^a Tetsuhiko Yorita,^a Masamichi Yoshioka^c and Masaki Takata^{a,b}

^aJapan Synchrotron Radiation Research Institute/SPring-8, 1-1-1 Kouto, Sayo-cho, Sayo-gun, Hyogo 679-5198, Japan, ^bCREST, Japan Science and Technology Agency, Japan, ^cSPring-8 Service, 2-23-1 Kouto, Kamigori-cho, Ako-gun, Hyogo 678-1205, Japan, ^dRIKEN, Harima Institute/SPring-8, 1-1-1 Kouto, Sayo-cho, Sayo-gun, Hyogo 679-5198, Japan, and ^eJAEA, Quantum Beam Science Directorate, 2-4 Sirane-Shirakata, Tokaimura, Naka-gun, Ibaraki 319-1195, Japan.
E-mail: tanaka@spring8.or.jp

Top-up operation allows SPring-8 to provide highly stable X-ray beams with arbitrary filling patterns. The implementation of top-up operation is described, with a focus on the simultaneous achievement of stability of stored current, beam orbit, purity of an isolated single bunch, and beam injection efficiency. Stored-current fluctuations have been routinely reduced to a level of 10^{-3} . Stored-beam oscillation on frequent beam injection, which was originally regarded as the most serious problem, has been successfully suppressed to a sufficiently low level that it never perturbs imaging experiments. Current impurities in nominally empty buckets have been reduced to a level of 10^{-9} over more than one week of operation, making possible the measurement of time-resolved spectra using high-current bunches. Finally, excellent injection efficiency, higher than 80%, is routinely obtained, even for small undulator gaps, which is critical for preventing radiation damage to insertion-device magnets and to reduce leakage radiation. The process of achieving highly stabilized top-up operation at SPring-8 and its utility for user experiments are described.

1. Introduction

The ideal synchrotron radiation source provides an intense, highly brilliant and extremely stable X-ray beam. Beam stability in turn requires (i) a stable electron beam orbit and emittance, (ii) stable current and (iii) stable X-ray optics. The generation of highly brilliant photon beams, however, demands high-density electron beams, which are difficult to provide with ideal stability. For example, at SPring-8, in the 3 nm rad emittance configuration with 0.2% coupling (Masaki & Takano, 2003; Tanaka *et al.*, 2000, 2002; Yabashi *et al.*, 2001),

the beam lifetime is about 100 h for a 0.1 mA bunch (Ohkuma *et al.*, 2003). This long lifetime is attained due to ultra-high-vacuum conditions and the high energy of the stored electron beam. However, increasing the bunch current by a factor of 10, to 1 mA, leads to the rapid degradation of the lifetime down to 10 h, due to increased electron–electron scattering at the higher electron density (Ohkuma *et al.*, 2003).

Top-up operation allows, in principle, a close approximation to an ideal synchrotron radiation source, with both high stability and high brilliance. In this mode, beam losses are continuously compensated by injections occurring every few

minutes, leading to an almost constant average current, or an essentially infinite lifetime. This is illustrated in Fig. 1, which shows the difference in average current in top-up and conventional operation at SPring-8. The precise level of current stabilization depends on the technical details of the injection beam handling, but at low injection currents variations can be reduced to the level of 10^{-4} . Such operation then enables (i) normalization-free scattering experiments, (ii) long-period and freely timed experiments without disturbance by beam injection and (iii) extreme stability in the photon beam position and energy in the experimental hutch, without fluctuations due to the thermal changes of X-ray beam optics. The beam injections are invisible for nearly all users.

First tests of top-up operation were carried out at the 1 GeV storage ring of SORTEC (Nakamura *et al.*, 1990) in 1990. Then, in 1996, Ueng and co-workers at NSRRC reported their results of a top-up test operation of ~ 6 h at the 5th European Particle Accelerator Conference. The stored current was kept in the range 194–200 mA, corresponding to a 3% deviation of the stored current. They concluded that realisation of top-up operation requires considerable reduction in the orbit variation caused by the beam injection, and in losses of the injected beam at the narrow-gap chambers of insertion devices (Ueng *et al.*, 1996). Meanwhile, the Advanced Photon Source (APS) regarded top-up operation as crucial from the beginning of the design phase, but a huge additional effort was needed for its realisation (Emery, 2001) because they, like SPring-8, followed

a conventional design. At the APS, top-up operation was realised in October 2001 (Emery & Borland, 2002) after six years of effort following the start of APS user operation. On the other hand, the Swiss Light Source (SLS) is the first synchrotron radiation source designed from the start for top-up operation. To reduce the injection beam loss, the SLS uses a low-emittance booster synchrotron which has the same circumference as the storage ring. In addition, to suppress the orbit variation of the stored beam, the beam injection point was selected in the middle of an 11 m-long magnet-free straight section. Also, a special injection scheme was designed, comprised of four identical bump magnets with a mirror-symmetrical arrangement (Böge, 2002; Lüdeke & Muñoz, 2002; Rivkin *et al.*, 1998). These design considerations made smooth beam commissioning with top-up operation possible at the SLS, with user operation in top-up mode beginning in the autumn of 2001. The successes at APS and SLS opened the door to top-up operation and made it an essential standard for brilliant synchrotron radiation sources, especially low-energy sources. Inspired by the successes of top-up operation at the above two facilities, most planned synchrotron radiation sources [SOLEIL (Level *et al.*, 2002; Loulergue *et al.*, 2002), SSRF (Liu, 2002), DIAMOND (Scott *et al.*, 2002), the Japanese UV and soft X-ray light source project (Nakamura, 2002)] consider top-up operation as a pre-requisite. Furthermore, many existing synchrotron radiation sources have started to investigate the introduction of top-up mode for user operation.

SPring-8 has succeeded in achieving a high-stability top-up operation by retrofitting. The purpose of this paper is to illustrate the process of the SPring-8 retrofitting, giving a better understanding of key technical factors for top-up operation. The merits of top-up mode are examined using results from several synchrotron radiation experiments.

2. Improvement of accelerator performance towards top-up operation with extreme stability

Although top-up operation has no limitations, in principle there are some notable technical hurdles that must be overcome:

- (a) orbit variation of the stored beam, which can disturb precise experiments;
- (b) de-magnetization of the permanent magnets of insertion devices (IDs) by bombardment of the injected beam;
- (c) deterioration of single bunch purity due to frequent beam injection.

Our target is top-up operation with extreme stability so that the essential properties of the stored beam (Tanaka, Aoki *et al.*, 2004) never deteriorate. We address each of these issues below.

2.1. Realisation of constant stored current

In order to keep the variation of the stored current under 0.1%, and to precisely preserve the beam-filling pattern in the storage ring, the injection beam current was stabilized by

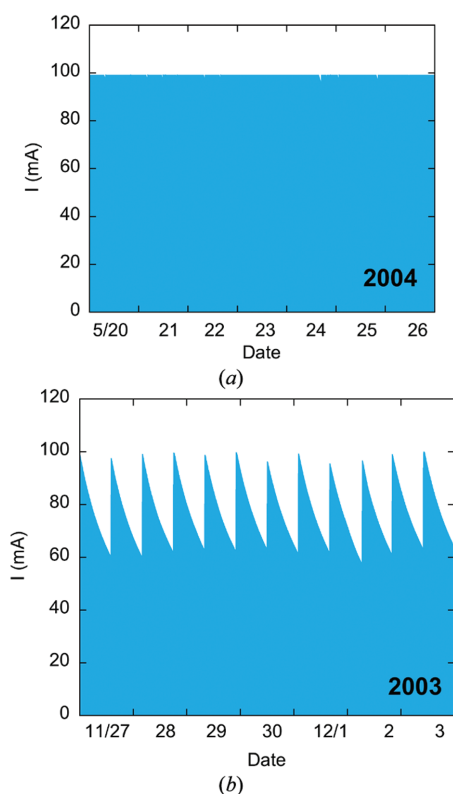


Figure 1 Difference in the stored-current stability between two operations over one week. The current stability of the SPring-8 storage ring (a) at top-up operation and (b) at conventional operation.

improving the long- and short-term stability of both the 1 GeV linac and 8 GeV booster synchrotron. Also, a system to precisely measure the individual bunch current was constructed to supplement the already-installed average-current monitoring system.

2.1.1. Stabilization of injection beam current. The current and energy of the beam from the linac were stabilized by improving the RF power and phase of the acceleration tubes, and installation of an energy compression system (Asaka *et al.*, 2002, 2004). Also, precise temperature control of the RF-cavity cooling water was introduced to stabilize the current of the ejected beam from the synchrotron. Both contributed to the long-term stability of the beam current injected into the storage ring. To suppress the shot-by-shot current variation caused by the single-bunch purification procedure in the synchrotron, an innovative timing system was introduced, which synchronizes the acceleration phases of the linac and synchrotron with different RF frequencies (Kawashima *et al.*, 2001).

As shown in Fig. 2, the 8 GeV SPring-8 storage ring and the 1–1.5 GeV NewSUBARU storage ring (Ando *et al.*, 1998) are both operated on the SPring-8 campus by time-sharing the 1 GeV beam from the linac. Fast switching of the beam routes between the two storage rings is thus necessary. To do this, the DC switching magnet was replaced by an AC magnet and the control system was modified. Consequently, the beam routes are now changeable within 10 s, including the status confirmation of all related equipment (Suzuki *et al.*, 2004). Recently, a new orbit feedback system (Yanagida *et al.*, 2004) was introduced to stabilize the beam paths to the two storage rings. This system is especially useful for long-term stabilization of the injection efficiency into NewSUBARU, which has a small acceptance.

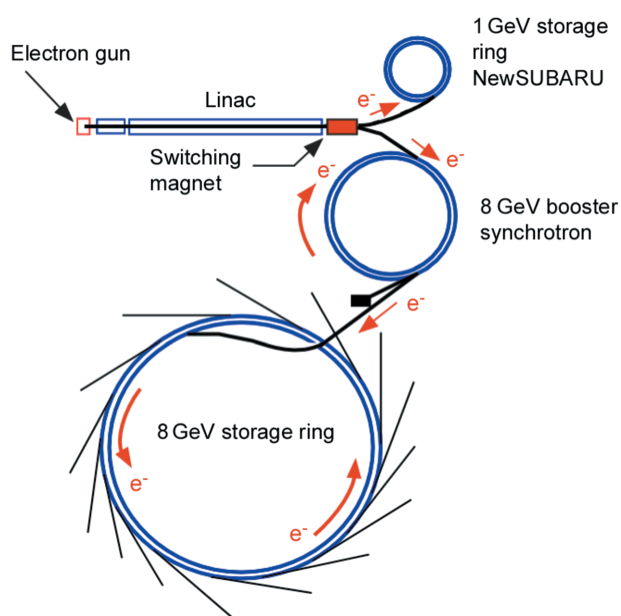


Figure 2
Schematic view of the SPring-8 accelerator complex. The complex is composed of a 1 GeV linac, 8 GeV booster synchrotron, 1–1.5 GeV NewSUBARU storage ring and 8 GeV SPring-8 storage ring.

2.1.2. Bunch-current monitoring system. SPring-8 operates in a number of different filling patterns, where only a precisely chosen subset of the 2436 RF buckets available are filled. This satisfies the demands of various timing measurements. However, for efficient use of beam time it is highly desirable that isolated filled-up buckets should have a higher current than those in bunch trains. This leads to a large difference in lifetimes in bunches with different filling due to different electron–electron scattering rates. Thus, a simple algorithm to calculate how many electrons should be injected into each bucket does not work if one wants to precisely preserve the stored current and filling pattern. To solve this problem a bunch-current monitoring system was constructed, where output signals from four button pick-ups of one beam-position monitor (BPM) are combined by a power combiner with a frequency range from 10 MHz to 2.5 GHz. The combined signal is read out by a fast, 20 G-sample s⁻¹, oscilloscope synchronized to the circulating electron bunches (Yoshioka *et al.*, 2003). This system can measure the bunch-current values of all of the 2436 RF buckets in about 25 s, with about 1% accuracy. After each beam injection the current in each bunch is measured by this system and the amount of beam for injection is determined accordingly.

2.2. Reduction of stored-beam oscillation caused by beam injection

Fig. 3 shows the injection bump orbit, injection beam orbit and injection magnets near the beam injection point. The electron beam ejected from the synchrotron passes through the beam transport line and then approaches the injection point (horizontally) from inside the ring. It is guided by three DC and one pulse septum magnets. The stored-beam orbit is bent like a bump to the side of the injection beam to shorten the distance to the injection beam (JAERI-RIKEN SPring-8 Project Team, 1991). This process reduces the oscillation amplitude immediately after the injection. The injection bump orbit is generated by four magnets in a trapezoidal configuration, as shown in Fig. 3. If there are no errors and no sextupole magnets inside of this bump orbit, it closes and never causes any oscillation of the stored beam due to the

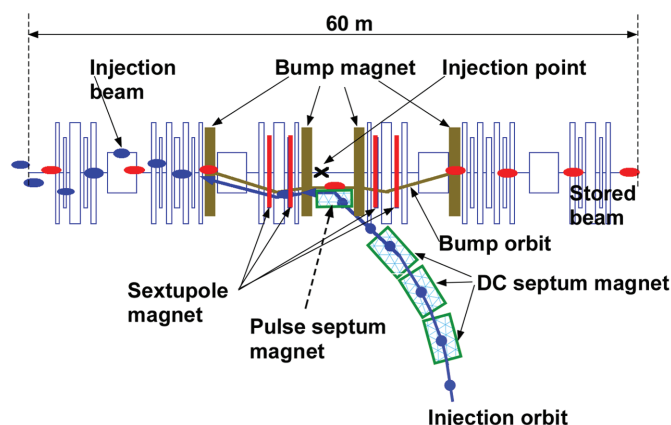


Figure 3
Schematic view of the beam injection system of the SPring-8 storage ring.

bump leakage. However, various kinds of errors cause stored-beam oscillation. Two methods are applied to reduce the stored-beam oscillation: suppressing the sources of oscillation and correcting the induced oscillation.

2.2.1. Suppression of sources for stored-beam oscillation.

(a) *Leakage field from the DC septum magnets.* Three DC septum magnets initially installed had large field leakage due to insufficient shielding and asymmetrical magnet-edges. This leakage generated a strong non-linear field on the central orbit. In particular, the horizontal field component was large and the estimated vertical oscillation due to the leakage field could be a few tens times larger than the vertical beam size. The three magnets were replaced by new ones with symmetrically shaped magnet-edges and good shielding performance. This reduced the field leakage, and the induced oscillation decreased to a tenth of the vertical beam size (Tsumaki *et al.*, 2004).

(b) *Sextupole magnets in the injection bump orbit.* Non-linearity of the sextupole field means that a sextupole magnet placed inside the bump orbit prevents the orbit from closing, for any oscillation amplitude. Since top-up operation was not considered at the design stage of SPring-8, four sextupole magnets were installed in the bump orbit to enlarge the dynamical stability as shown in Fig. 3. These caused oscillation with an amplitude of 1 mm or more. On careful investigation we found that the minimum leakage of the bump orbit, in the lowest order, does not depend on the bump amplitude (Tanaka *et al.*, 2005). By using this minimum condition, the amplitude of the induced oscillation can be reduced to a few tens of micrometres, as shown in Fig. 4, if the waveform of the bump field is a perfect half-sine. To realise this minimum condition, and keep a large dynamic aperture for the stable beam injection, the unit cell of the ring was expanded from one Chasman-Green cell to two, and the number of sextupole

families was increased from four to six by changing the cabling of the sextupole magnets (Tanaka, Ohshima *et al.*, 2004).

(c) *Improvement of waveform uniformity of injection bump magnets* (Ohshima *et al.*, 2004). Four bump magnets, each having a half-sine waveform, with a time width of about 8 μs , generate the injection orbit bump, which peaks at about 4 μs . If the field waveforms of all magnets are not the same shape (related by a similarity transformation), or not perfectly synchronized, there will be leakage of the bump orbit which induces stored-beam oscillation, even without non-linear magnets in the bump orbit. The impedances of the four bump magnets were adjusted assuming that the magnetic field waveform was the same as the current waveform. However, the four field-waveforms estimated by the real beam response measured using a single-pass beam position monitor (SPBPM) were not identical. A large disturbance was noted in the latter part of the waveform that, on detailed investigation, was found to be a result of eddy currents in the stainless steel endplates. The endplates are used to fix the magnet yoke made by piling thin silicon steel sheets (thickness of 0.1 mm) covered by an insulator film. Two types of bump magnets of different lengths were used so the effects of eddy currents on the integrated fields of the two were not identical, breaking the required symmetry. To prevent the eddy-current generation, four new magnets with glass-polyester-mat endplates were manufactured. Tuning was carried out by using an integrated field-waveform measured by a long coil covering the longitudinal field region. The similarity of the field waveforms was then much improved, as shown in Fig. 5. In parallel, synchronization of the excitation timing of the four magnets was adjusted. Final tuning was then carried out using the real beam response.

(d) *Bump magnet tilt error* (Ohshima *et al.*, 2004). Vertical oscillation of the stored beam during beam injection was observed to have a strong correlation with the waveform of the bump magnet. This suggested that horizontal leakage directly generates the vertical oscillation through transverse coupling, with magnet tilt around the longitudinal axis being a probable source. Using the vertical oscillation data measured using a SPBPM, the tilt angles of the four bump magnets were estimated, and then corrected. This reduced the vertical oscillation by a factor of two, and the clear correlation with the waveform of the bump magnet disappeared.

2.2.2. Correction of residual beam oscillation. After completing the corrections discussed above (§2.2.1), it became reasonable to consider correcting the residual oscillation using a wide-bandwidth power supply. The horizontal and vertical oscillations caused by the beam injection were measured using a SPBPM and investigated in detail to determine the best places for a single horizontal corrector and a single vertical corrector. Then, the aluminium vacuum chambers were replaced by ceramic ones and fast correction magnets were installed. The current waveforms for the correction magnets were experimentally obtained by analysis of the beam oscillation data measured using a SPBPM. Feed-forward correction systems for the horizontal and vertical oscillations were constructed and each system had an arbitrary waveform

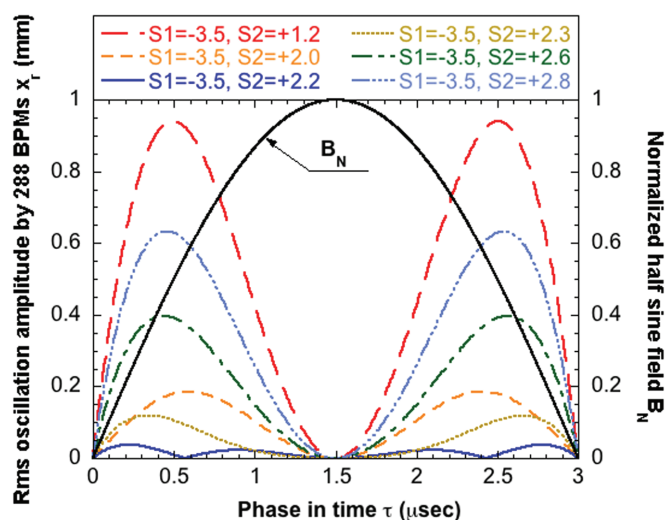


Figure 4 Calculated bump leakage variation as a function of the ratio of two sextupole strengths in the bump orbit. Here the strengths of the bump magnets are adjusted to close the bump orbit at its peak amplitude in consideration of sextupole non-linearity. A pulse width of 3 μs was used in the calculation.

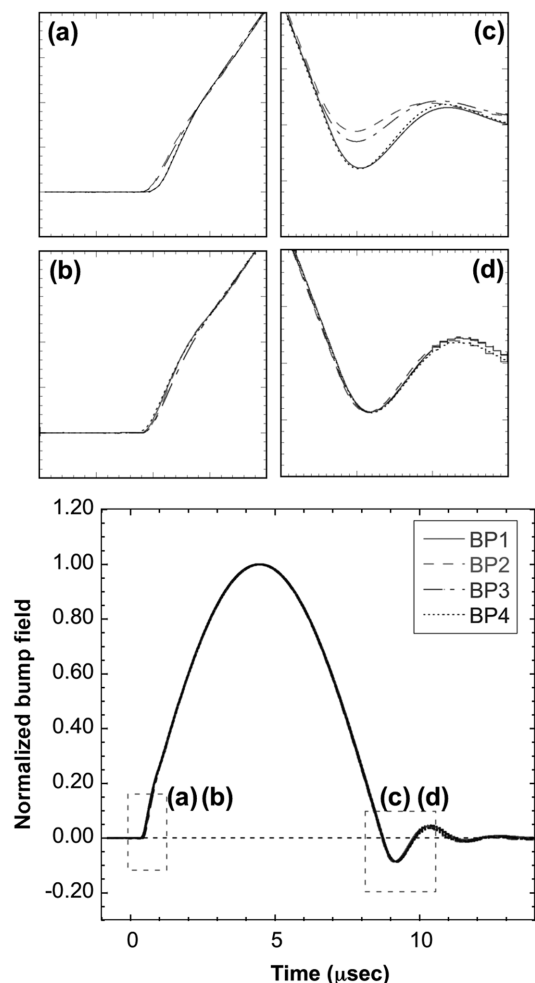


Figure 5 Similarity improvement of four bump-field waveforms before and after the improvement. Parts (a) and (b) show the magnified rising parts of the waveforms before and after the improvement, respectively. Parts (c) and (d) show the magnified falling parts of the waveforms before and after the improvement, respectively.

generator used to generate a low-level signal that was then amplified and fed to the fast correction magnet (Ohshima *et al.*, 2004).

2.3. Reduction of injection-beam loss

Injection-beam loss is a complicated non-linear process involving two coupled modes of a circulating electron, betatron and synchrotron oscillations. This was investigated with particle tracking simulations using a precise ring model with a realistic error distribution (Soutome *et al.*, 1999; Tanaka *et al.*, 2001). The simulations showed that the main causes of injection-beam loss were the large amplitude of the horizontal oscillations of the injection beam and the high linear chromaticity of the storage ring (Takao *et al.*, 2004).

2.3.1. Reduction of horizontal oscillations of the injected beam. The horizontal beam size at the beam injection point was about 1.7 mm (r.m.s.) which is not negligible compared with the 10 mm coherent oscillation amplitude of the injection beam. To reduce the horizontal beam size, we installed a

collimator using two beam scrapers (with a 90° phase difference for the horizontal betatron oscillation) in the beam transport line from the synchrotron (Fukami *et al.*, 2004). This system cuts a square shape from the horizontal phase space of the injected beam: if the tail of the injected beam is cut at 1 standard deviation, the emittance is reduced by a factor of ten while 47% of the beam is preserved. Furthermore, owing to the smaller beam size, the injection orbit can be shifted by about 2 mm to the wall of the pulse septum magnet. The collimator system works effectively to reduce both the average and maximum oscillation of the injection beam.

2.3.2. Reduction of operating chromaticity. The various in-vacuum IDs in the storage ring and their narrow vertical gaps create a large low-frequency impedance for the circulating beam. Hence, if the chromaticity is chosen to be small and positive, as the number of in-vacuum IDs increases, beam instabilities are excited by the vertical narrow gaps. In 2004, the chromaticity (ξ_x, ξ_y) in the user operation was set to large values, (+8, +8) to suppress the instabilities by enhancing Landau damping. To operate all beam-filling patterns with low chromaticity, a bunch-by-bunch feedback system (BBF) with a field programmable gate array was developed (Nakamura *et al.*, 2004). Using this system the operating chromaticity was reduced from (+8, +8) to (+2, +2).

The injection-beam loss was reduced markedly by combining collimator and low chromaticity operation. Fig. 6 shows the dependence of the injection efficiency on the half-width of two scrapers in the collimator system with low chromaticity, (+2, +2). When the gaps of all in-vacuum IDs are closed to the minimum values, an injection efficiency of about 90% can be retained by closing the full-width of the two scraper gaps to 1 standard deviation of the injection beam. However, fluctuation of the injection efficiency increases as the scraper gap is closed. Since the cause of this is presently unclear, the full width is set to 2 standard deviations of the injection beam, so about 80% efficiency is assured under standard operating conditions.

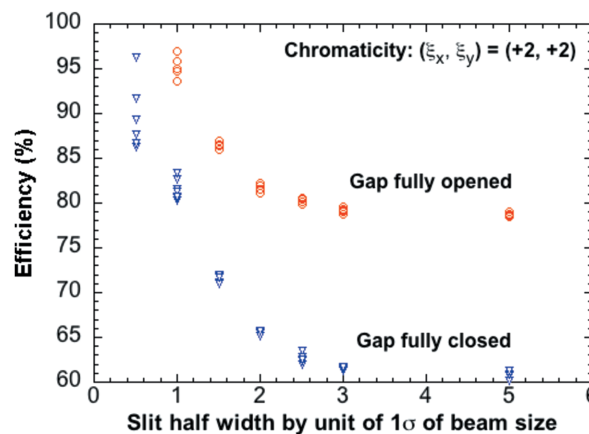


Figure 6 Dependence of the injection efficiency on half-width of a pair of horizontal scrapers. The units of the horizontal axis are 1σ of the horizontal beam size at the scraper.

2.4. Generation of high-purity isolated bunches

Isolated single bunches are needed for some classes of experiments, such as nuclear resonant scattering. Here the emphasis is on providing a single filled-up RF bucket, with no ‘dust’ electrons in nearby buckets, so that the X-ray pulse, some 40 ps in FWHM for a 1 mA bunch, is truly isolated. To quantify this, we define the bunch purity (impurity) as the number of target single-bunch (dust) electrons normalized to the nearby (target single) bunch. In top-up operation, where the stored current is kept constant by frequent beam injections, the conservation of good purity over long operation periods is challenging.

2.4.1. Purification of single bunches in booster synchrotron. Owing to the high ring energy, 8 GeV, there is no path for electrons in one RF bucket to diffuse into another once they are in the storage ring: radiation damping, which is fast compared with in a low-energy ring, forces circulating electrons with large energy deviation to return to the identical RF bucket or be lost by colliding with the vacuum chamber wall. Thus, the purity is kept constant during intervals between beam injections, and the goal is then not to degrade the purity by the frequent injections. This requires either cleaning the beam in the storage ring itself, or cleaning the beam before injection. As cleaning the beam in the storage ring tends to interfere with user operation, the beam is cleaned in the synchrotron. Thus we have been gradually improving the RF knock-out system (RFKO) that was installed at SPring-8 since its first operation. This system consists of an arbitrary waveform generator, high-power amplifiers and stripline-type kicker (Suzuki *et al.*, 2000). Optimization and stabilization of cooling water temperature of the RF cavities, betatron tunes, chromaticity and acceleration voltage contributed to the performance improvement. The new timing system described in §2.1.1, which synchronizes the acceleration phases of the linac and synchrotron to ~ 10 ps, also contributed to the improvement. Thus we realised the stable generation of single bunches with a purity of 10^{10} in the synchrotron (Aoki *et al.*, 2003).

2.4.2. Precise measurement of single-bunch purity. A measurement system with high resolution is necessary for monitoring the purity during user operation, and for precise tuning of the RFKO system. Our purity measurement system, installed at the accelerator beam diagnosis beamline, BL38B2 (Tamura & Aoki, 2004), uses visible-light photon counting.

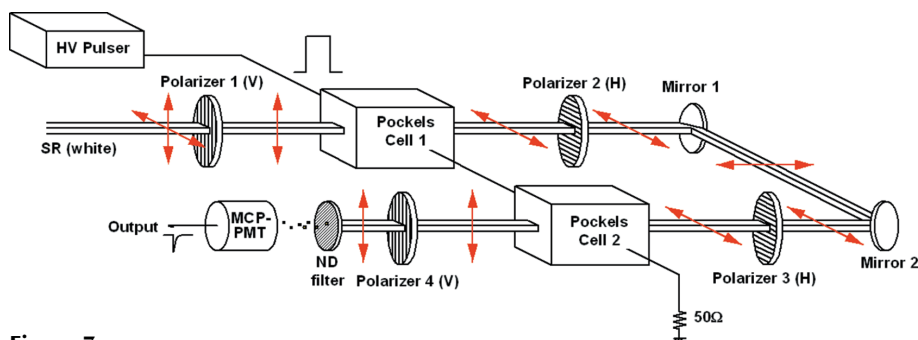


Figure 7
Schematic view of the monitoring system for purity measurements.

Task \ Stage	First stage (Phase 0)	Second stage (Phase I)	Third stage (Phase II)
Machine R&D	[Timeline bar from Phase 0 to Phase I]		
Beam tuning & test	[Timeline bar from Phase 0 to Phase I]		
Influence check of beam injection to experiments	[Timeline bar from Phase 0 to Phase I]		
Trial use of top-up	[Timeline bar from Phase I to Phase II]		
Performance check by users	[Timeline bar from Phase I to Phase II]		
Survey of radiation leakage	[Timeline bar from Phase I to Phase II]		
Top-up with constant current	[Timeline bar from Phase II to the end]		

Figure 8
The three stages of top-up operation.

We used two pockels cells as a fast photon shutter to attenuate the signal from the filled-up bunch (see Fig. 7). Using a microchannel-plate-type photomultiplier tube with careful suppression of stray light reflections, an attenuation of $\sim 10^5$ has been achieved. The impurity of the bunches in front of and behind the filled-up bunch can be measured in 30 min with a resolution of 10^{-10} .

3. Performance of SPring-8 top-up operation

Top-up operation was achieved in three stages as shown in Fig. 8. Phase 0 was a preparation period where the relevant machine performance was investigated, and R&D of required systems were carried out off-line. In the latter half of Phase 0, study and tuning with beam were also performed. After each improvement of the machine performance, the influence of beam injection on various types of experiments was investigated. Phase I was a trial period. The beam was injected at the usual refilling times (either every 12 or every 24 h) but with beam shutters open, and without opening the ID gaps. Experimental users were free to continue recording data, or not, during beam injection. In this phase the stored beam oscillation caused by the beam injection had to be suppressed to keep high injection efficiency. This was resolved by combining low chromaticity operation with BBF and optimization of the linear and non-linear optics. Finally, after examination of radiation safety, Phase II (top-up with a constant beam current) was started on 20 May 2004. Here the beam is injected at one (five) minute intervals in several (multi-) bunch operation (Tanaka, Aoki *et al.*, 2004). To realise the top-up operation of both of the storage rings on the

SPring-8 campus, a fast-switching dipole magnet was introduced to change the two beam routes quickly. In the following we summarize the achieved beam performance of the SPring-8 top-up operation.

3.1. Radiation leakage in top-up operation

The leakage of γ -rays and neutrons in top-up operation was the same as without top-up. This was demonstrated

by thorough investigation, especially around optical hitches of beamlines, with the photon beam shutters opened and the gap of the in-vacuum undulators fully closed. Also, the radiation level is routinely measured in many places, *e.g.* on the ceiling of a machine tunnel, at the sidewall of a machine tunnel, around the beam injection section and at various places in the experimental hall. These measurements confirmed that the amount of leakage of γ -rays and neutrons during top-up operation is at the same level as for conventional operation.

3.2. Stability of stored-beam current

The stability of the stored-beam current in Phase II is clearly seen from Fig. 9, where the beam current of the SPring-8 storage ring is plotted together with that of the NewSUBARU ring. Fig. 9(a) shows the stability over 5 d for the SPring-8 storage ring operated in multi-bunch mode with beam injected every 5 min. The deviation of the stored current is smaller than 0.1% over long periods, except when there were problems with the injector. The decays in the current of NewSUBARU were not due to the injector troubles but to the operational demands, *e.g.* operation with a stored energy of 1.5 GeV or machine study. To keep the stored current constant in NewSUBARU we checked whether the beam injection was necessary or not every 8 s. Fig. 9(b) shows the short-term stability of the stored current of both rings over 1 h on 2 October 2004. Since the SPring-8 storage ring has priority over NewSUBARU in using the linac, the beam current of NewSUBARU shows a dip every 5 min. The stability of the current is nevertheless better than 0.3%. The beam current of each isolated single bunch (bunch current) is also kept constant in the SPring-8 storage ring. This is seen from Fig. 9(c) where the deviation of the bunch currents of 18 isolated bunches is plotted over one week. The filling pattern was ‘2/21 bunch-train and 18 isolated bunches’, in which 2/21 of the RF buckets are occupied by a train of bunches and 18 isolated single bunches are equally spaced around the ring as shown in Fig. 10. The deviation of the beam current of isolated bunches is smaller than 3%.

3.3. Stability of stored beam at beam injection

The oscillation of the stored beam caused by beam injection was measured using SPBPMs synchronized to the beam injection (see Fig. 11). Analysis of the data shows that the r.m.s. horizontal and vertical amplitudes of the residual oscillations are about 100 μm and 6 μm , respectively. Considering the distribution of betatron functions along the ring, the horizontal amplitude of the residual beam oscillation is suppressed to about one-third of the horizontal beam size at insertion devices, and the vertical amplitude to one-half of the vertical size (Ohshima *et al.*, 2004; Tanaka, Aoki *et al.*, 2004).

To confirm that the achieved stability of the stored beam is sufficient for precise experiments, the fluctuations of the X-ray beam caused by injection were measured at BL39XU (Hayakawa *et al.*, 1998). The intensity of the X-ray beam downstream of the monochromator was measured using a

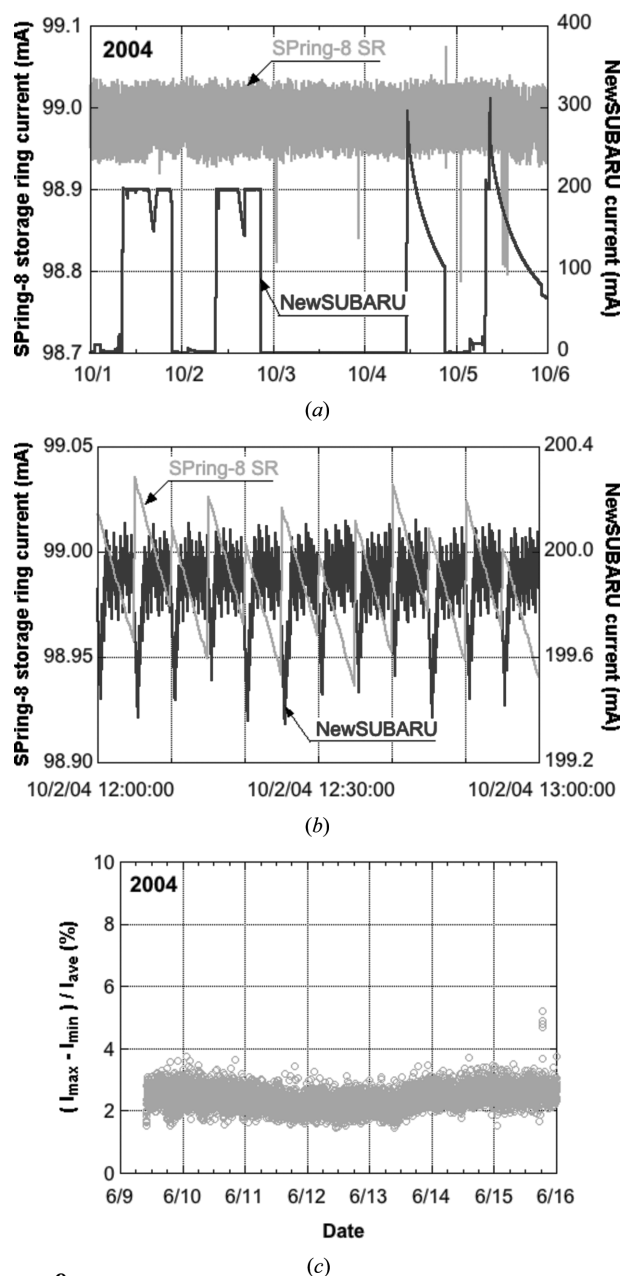


Figure 9 Stored-current stability of two storage rings on the SPring-8 campus. (a) Long-term stability over 5 d, (b) short-term stability of 1 h, and (c) the current uniformity of 18 single bunches over one week. The vertical axis of (c) represents a peak-to-peak variation of 18 single-bunch current data normalized by the average of the 18 bunch current data.

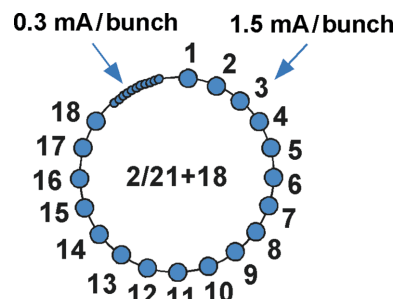


Figure 10 Schematic view of the filling pattern ‘2/21 bunch-train and 18 isolated bunches’.

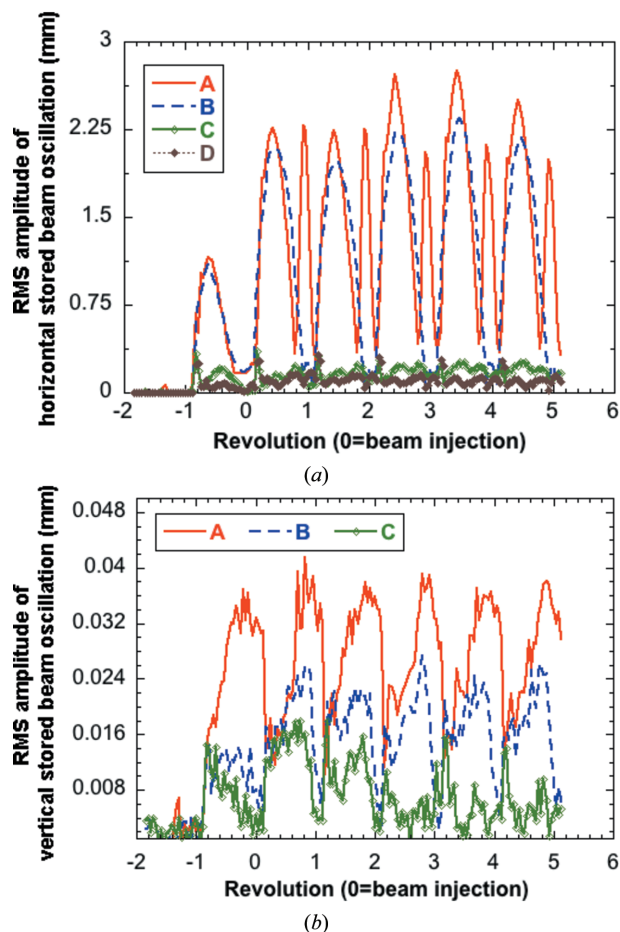


Figure 11
 RMS amplitudes of (a) horizontal and (b) vertical stored beam oscillations caused by beam injection at each improvement step. (a) A: before the correction; B: by the bump field adjustment; C: by the bump field adjustment and sextupole field optimization; D: by the bump field adjustment, sextupole field optimization and feed-forward correction. (b) A: before the correction; B: by the tilt error correction; C: by the tilt error correction and feed-forward correction.

silicon PIN photodiode. The output current of the photodiode was converted into a voltage signal by a fast amplifier with a 2 μ s rise/fall time and was then recorded by a digital storage oscilloscope with a 1 μ s time resolution. The time variation of the X-ray beam position and profile were deduced from a series of intensity waveforms obtained by varying the XY slit position at the front-end (29 m from the source). The X-ray intensity fluctuation due to electron beam injection before and after the bump leakage suppression is shown in Fig. 12 (see §2.2). Before suppression, the X-ray intensity dropped by 70% just after injection. Then, the intensity was recovered in 20 ms with oscillations at a 4.8 μ s period. However, after suppression of the leakage, intensity loss due to injection was reduced to 15% and the time for recovery was reduced to 10 ms. This shortening of the recovery time is due to the BBF system. Fig. 13 shows the variation of the centre of the X-ray beam position at the front-end XY slit. The X-ray beam position fluctuated by $\pm 170 \mu$ m in the horizontal and $\pm 200 \mu$ m in the vertical directions before leakage suppression. After leakage suppression, the amplitude of the X-ray beam fluctuation was

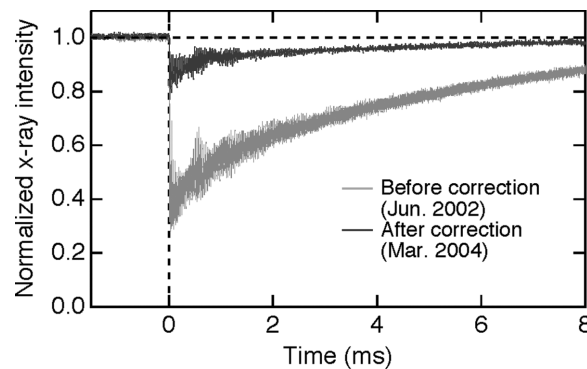


Figure 12
 Drops in X-ray intensity by the beam injection measured at BL39XU before and after the bump leakage suppression.

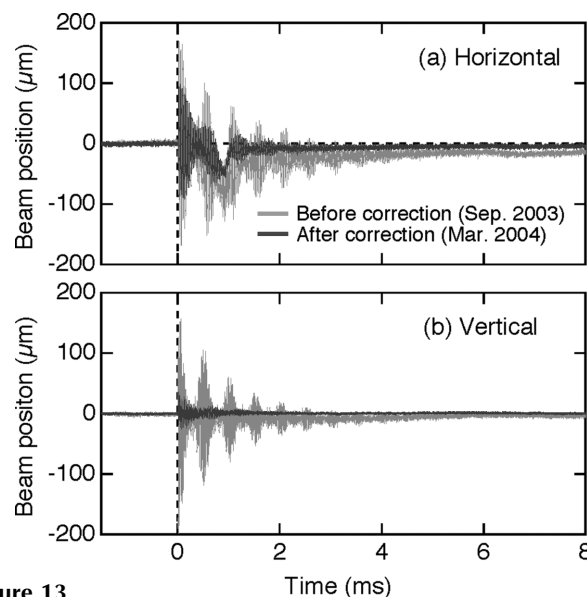


Figure 13
 Variation of (a) horizontal and (b) vertical X-ray beam positions at the BL39XU front-end slit caused by the beam injection. The grey (black) lines show the beam position before (after) the bump leakage suppression.

reduced to $\pm 100 \mu$ m in the horizontal and $\pm 50 \mu$ m in the vertical, as seen in Fig. 13. The improvement in the vertical is particularly noteworthy. The X-ray beam size at the XY slit position was 1300 μ m (horizontal) \times 500 μ m (vertical) in FWHM so the observed fluctuations of the beam position were less than one-tenth of the beam size. The beam returned to the original position within 1.5 ms after the injection. The duration of the fluctuation in beam position is then less than 0.01% of the total operation for one injection per minute.

The influence of the stored-beam stability on the reliability of imaging data was investigated at BL47XU with the two setups that are quite sensitive to X-ray source fluctuations. The X-ray beam position at the end-station was measured with a high-speed X-ray camera. The camera pixel size was 20 μ m, exposure time 5 ms and frame rate ~ 200 Hz. Fig. 14 shows the motion of the horizontal centre of mass before and after leakage suppression. The shifts of intensity (70%) and position (40 μ m) before leakage suppression were entirely removed after the leakage suppression.

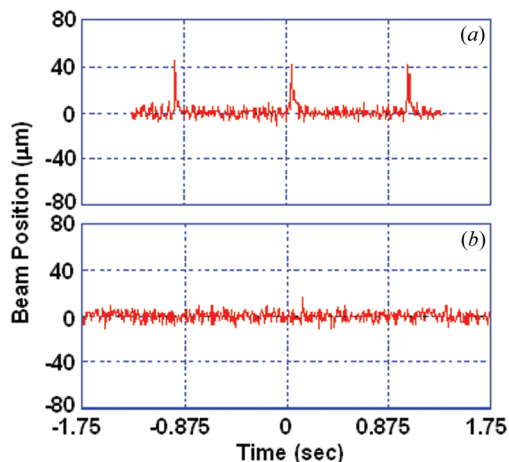


Figure 14 Variation of horizontal X-ray beam position measured at BL47XU (a) in December 2002 before the improvement and (b) in February 2004 after the improvement.

We also examined the influence of top-up injection on a scanning microscope experiment using a Fresnel zone plate (FZP) with a $0.5\ \mu\text{m}$ beam spot (Suzuki *et al.*, 2001). The distance between the source and FZP was about 50 m, the FZP focal length was 200 mm (at 10 keV) and a slit located at 29 m from the source was used as a virtual source. Fig. 15 shows transmitted images of the sample obtained using this system. The scan pitch was 150 nm, the rate was about 4 Hz per point and the total time required for one scan was about 45 min. The images are not normalized by the incident X-ray intensity. The upper image was measured before the leakage suppression and shows intensity variations of about 5%. The lower image, measured after the leakage suppression, shows negligibly small intensity fluctuation. These results show that the achieved stability of the stored beam is extremely good, and should not influence any planned imaging experiments.

3.4. Injection-beam loss

The efficiency of beam injection is measured by using a beam charge monitor installed in the transport line and a DC current transformer installed in the storage ring. The beam charge monitor is located at a position close to the injection point and measures the beam current injected into the storage ring. The injection efficiency is calculated by comparing the two after a calibration using several current monitors during on-axis injection. In an ideal on-axis injection, there is no oscillation of the injected beam and the amount of beam loss is negligibly small. Fig. 16(a) shows fluctuations of the injection efficiency over 6 d of user operation (Tanaka, Aoki *et al.*, 2004). The full widths of the two scraper gaps in the transport line were set to 2σ of the horizontal beam size. The BBF system was switched on, the horizontal and vertical chromaticity values of the ring were adjusted to +2, and the ring optics was of the oscillation-suppressed type so that the oscillation of the stored beam was suppressed during the injection. An average efficiency of more than 80% was achieved. Owing to the high and stable injection efficiency, any degradation of

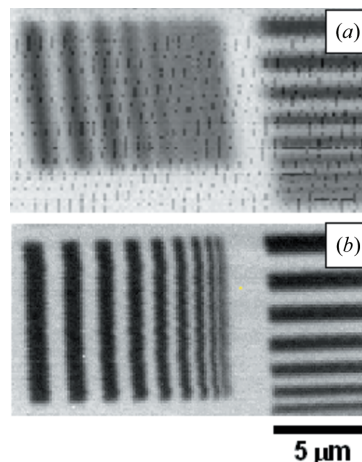


Figure 15 Transmission images of a test pattern obtained at BL47XU using a scanning X-ray microscope, measured (a) in October 2002 before the improvement and (b) in June 2004 after the improvement.

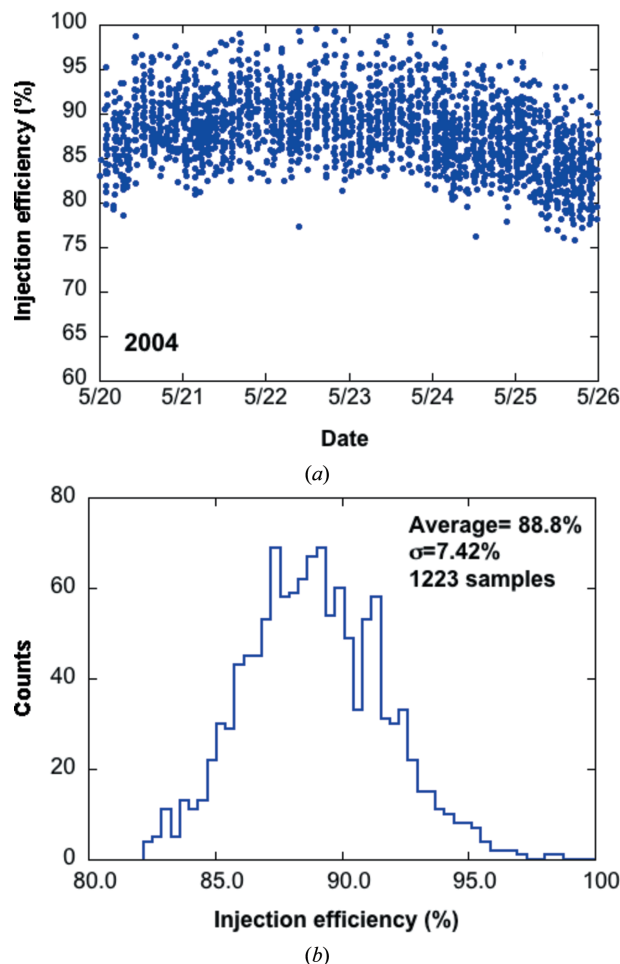
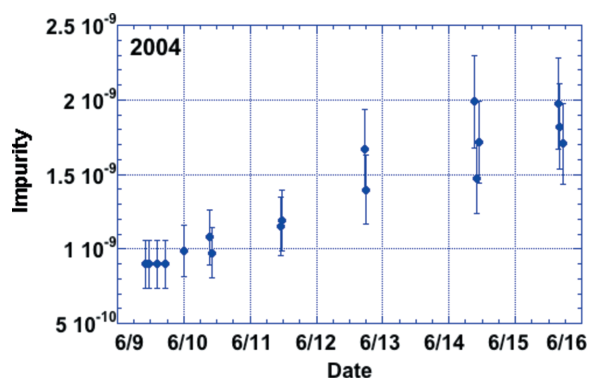
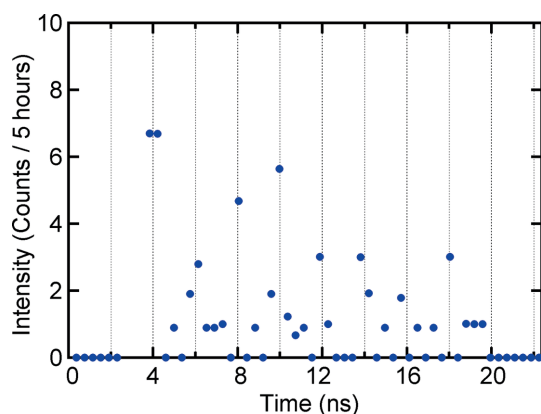


Figure 16 Variation of injection beam efficiency. (a) Long-term variation over 6 d and (b) statistical distribution of the injection beam efficiency for 1 d.

ID permanent magnets has not been observed over about two years of operation. Long-term drift can be seen and is presently being investigated: it has no correlation with the gap status of the insertion device but may be due to a slow change


Figure 17

Variation of the single-bunch impurity over one week. The impurity of the RF bucket behind the target single bunch was measured at BL38B2 by the photon-counting system. Error bars represent a statistical error in the measurement.


Figure 18

Measured time spectrum of noise in top-up operation with 203 bunch mode. The data were measured using an avalanche photodiode at BL09XU on 3 July 2004. The total counts from the 203 bunches in this measurement period were 8×10^{10} and the averaged impurity can be estimated by normalizing the measured counts by 8×10^{10} . The reference of the horizontal axis (relative time) is the middle of each single bunch. The separation of the RF buckets is 2 ns and each dashed vertical line represents the centre of the corresponding RF bucket in relative time.

of injection beam passage through the transport line. Fig. 16(b) shows a typical statistical distribution of injection efficiency over 1 d. Although the efficiency depends on the gap value of the insertion devices, the averaged efficiency on this day was about 90%. As seen from Figs. 16(a) and 16(b), the measured value of injection efficiency shows a deviation of about $\pm 5\%$. The main source of this deviation is thought to be the noise of the beam charge monitor induced by exciting pulsed magnets for beam injection.

3.5. Purity of isolated bunches

Fig. 17 shows the measured impurity (inverse of purity) of an isolated bunch over one week of user operation. In this measurement the RF bucket behind the target bunch was chosen. The filling pattern was ‘2/21 bunch-train and 18 isolated bunches’ (see §3.2), and the current of each isolated bunch was 1.5 mA. The total current injected into each isolated bunch over the period of this measurement was about

15 mA or 5×10^{11} electrons. As seen from the figure, the impurity increased from 1×10^{-9} to 2×10^{-9} or the purity decreased from 1×10^9 to 5×10^8 after one week, so the number of electrons in the monitoring RF bucket increased by about 50. From this we estimate that the average purity (impurity) of an injected beam from the booster synchrotron is about 1×10^{10} (1×10^{-10}) (Tanaka, Aoki *et al.*, 2004).

Fig. 18 shows the impurity distribution between the filled-up bunches over 5 h, as measured at BL09XU during the top-up operation in 203 bunch mode. Results from all 203 bunches were summed. The accumulated total intensity in the filled-up bunches is 8×10^{10} . Therefore the measured impurity of each bunch after the second RF bucket or 4 ns from the filled-up bunch is better than 2×10^{-10} . It should be noted that the data away from the dotted line are noise arising from cosmic rays and from the time resolution of 0.3 ns.

4. Impact of the top-up operation to synchrotron radiation experiments

The merits of the top-up operation for synchrotron radiation experiments include the following.

(a) Increased time-averaged photon flux: this is due both to the lack of current decay losses and to no longer losing time to injections and the attendant optical stabilization. Consequently, for experiments in multi-bunch mode, top-up operation provides about 1.5 times higher intensity, while, for the isolated bunches in few-bunch modes where decay times are faster, the gain is more like a factor of 3.

(b) Current stability better than 0.1%: the constant heat loads on optics, including the beamline monochromators, allow monitor-free measurements.

(c) No experimental interruptions from refilling: the operation without breaks for electron refilling allows planning of long and stable measurements.

In this chapter we describe some examples of the experimental progress achieved by our top-up operation, which, for general user operation, began in May 2004. The effects of intensity fluctuation due to the injection were invisible in all planned user experiments and tests. Imaging measurements, high-resolution X-ray computed microtomography, photoelectron emission microscopy, photoelectron spectroscopy, and magnetic circular dichroism experiments show that top-up has no influence on the data reliability. As for ultra-high-resolution time-resolved experiments in the future, the data quality might degrade owing to the present intensity fluctuation. For such cases, however, injection trigger signals (hard wire, TTL level, ON at 1 ms before the moment of injection, OFF at 11 ms after) and a message system to serve notice of the next injection (computer command, answer back the remaining time until next injection) are available.

4.1. Step-scan diffraction experiments

Step-scan measurements (*i.e.* measuring the scattered X-ray intensity by, for example, changing the scattering angle of the detector) are widely used for many experiments. Generally

they are corrected by monitoring the incident X-ray intensity. However, top-up operation succeeded in eliminating the need for a monitor in diffraction experiments on disordered materials at the high-energy X-ray diffraction beamline BL04B2. Diffraction data of amorphous silica measured with 61.6 keV X-rays are shown in Fig. 19. Since the scattered intensity drastically decreases with an increase in the scattering angle, as shown in the figure, it is necessary to obtain the correct intensity profile in the high-angle region to place the observed data on an absolute scale. In order to obtain the correct intensity profile of disordered materials up to large values of scattering vector Q , the measurement is performed using θ - 2θ step scans with an intrinsic Ge detector over a period of 4–

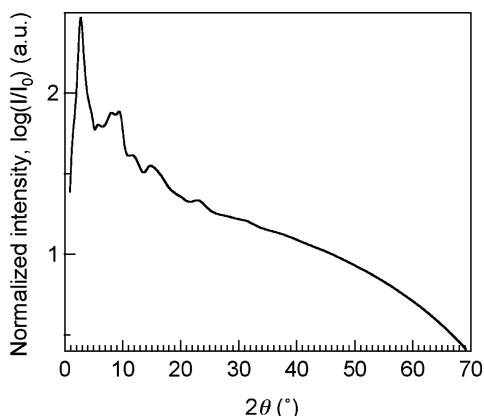


Figure 19
X-ray diffraction pattern of amorphous silica measured at BL04B2.

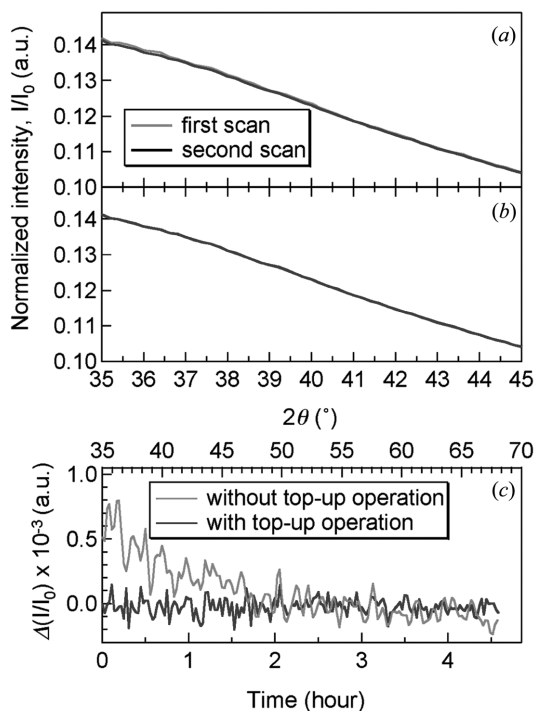


Figure 20
X-ray diffraction patterns of amorphous silica measured at BL04B2 (a) for conventional operation and (b) for top-up operation. (c) Differences in scattering intensity between the first and second scans.

12 h. Therefore the incident flux of photons should have a high stability for the long time scan over a wide range of Q .

Fig. 20(a) shows high-angle data of amorphous silica measured under the conventional non-top-up mode. The differences in scattering intensity between the first and second scans are due to the fluctuation of the incident beam flux. On the other hand, the two intensity profiles measured under top-up mode are almost identical, as shown in Fig. 20(b). Fig. 20(c) shows the difference in scattering intensity between the first and second scans. For the top-up mode case, the difference is almost equal to zero, which demonstrates that the heat load to the monochromator of BL04B2 remains equal to a steady value owing to the constant stored-beam current of the storage ring.

In order to investigate the advantage of top-up operation on the structural analysis of disordered materials, both sets of diffraction data are normalized to the total structure factors, $S(Q)$, and Fourier-transformed to the total correlation functions in the real space, $T(r)$. The structure factor $S(Q)$ of amorphous silica, obtained in top-up mode, exhibits proper oscillations at around unity up to 32 \AA^{-1} , as shown in Fig. 21(a), whereas that obtained in conventional mode exhibits a spurious drift from unity in the high- Q region ($Q > 20 \text{ \AA}^{-1}$), producing significant artificial ripples in the correlation function, $T(r)$, as shown in Fig. 21(b), at $r < 1 \text{ \AA}$ and $r > 4.5 \text{ \AA}$.

The top-up operation of SPring-8 allows us to measure very precise diffraction data of disordered materials up to high Q .

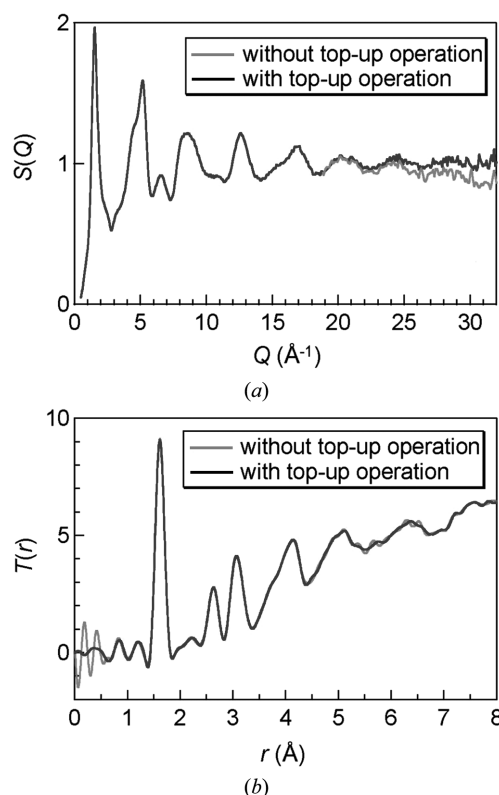


Figure 21
(a) Total structure factor $S(Q)$ and (b) total correlation function $T(r)$ of amorphous silica measured at BL04B2.

It is particularly well suited to detecting small differences in structure between two isotopic substituted amorphous samples such as isotopic quantum effects in water (Hart *et al.*, 2005).

4.2. X-ray spectroscopy experiments

The extremely stable stored current in the successful top-up operation should provide definite benefits for X-ray spectroscopy experiments. The quality of spectroscopy data does not solely depend on the intensity of the light source but also strongly on the stability of the light source and data-acquiring system. In this context the important benefits brought from the top-up operation are improved stabilities in (a) the electron beam orbit, (b) X-ray optics and (c) feedback control of the beamline monochromator (Nishino *et al.*, 2003).

These benefits improved the accuracy and reliability in X-ray spectroscopy experiments. For instance, in X-ray magnetic circular dichroism (XMCD) spectroscopy measurements at BL39XU (Maruyama, 2001), a tiny XMCD signal, a few parts in 10^5 of the normal X-ray absorption, is routinely obtained in top-up mode. An excellent example is the observation of clear XMCD spectra of the order of 10^{-5} , measured at the Cu *K*-edge for a $[\text{Co}/\text{Cu}_{0.9}\text{Ni}_{0.1}]_{50}$ multilayer (Ishiji *et al.*, 2005). These signals originate from a tiny magnetic moment ($\sim 0.02 \mu_B$ per atom) of the Cu layer. Such a high accuracy will provide the opportunity to investigate weak magnetization induced in non-magnetic elements in magnetic/non-magnetic heterostructures or in organic magnets by X-ray spectroscopy.

4.3. Nuclear resonant scattering experiments using special bunch modes

Nuclear resonant scattering of synchrotron radiation is useful for Mössbauer spectroscopy under extreme/diffraction conditions and for isotopes for which it is difficult to prepare radioactive sources or samples. Nuclear resonant inelastic scattering is also an important technique for studying the element-specific vibrational density of states. Top-up operation is extremely useful for these experiments for several reasons. One is that special bunch modes with interval time between bunches suitable for nuclear lifetimes, which typically range from ns to μs , are required to measure time spectra. Another reason is that the counting rates of nuclear resonant scattering are not generally so high because of the narrow energy widths which typically range from neV to μeV . Therefore, the increase in the integrated intensity due to top-up operation opens new possibilities in nuclear resonant scattering experiments.

One example is the measurement of the site-specific vibrational density of states developed at SPring-8 (Seto *et al.*, 2003). This technique gives site-specific information which cannot be obtained by other general methods. However, it requires several days to record a data set, even under ambient conditions. The integrated intensity in each single bunch used in this bunch mode has increased almost three times by top-up operation considering the injection time and the adjustment time after the injection. Therefore advanced measurements of

more dilute samples or under extreme conditions could be expected in the future. Another example is improved energy resolution for nuclear inelastic scattering experiments. The energy resolution should be determined by a trade-off between the resolution and the intensity, although higher resolutions are always required in the nuclear inelastic scattering experiments, especially when resolving complicated vibrational modes in macromolecules such as enzymes and proteins. A suitable resolution, which depends on the individual samples, was improved by more than twice owing to the top-up operation.

4.4. Inelastic X-ray scattering experiments

Top-up operation was greeted with great enthusiasm by users and staff of BL35XU, the beamline for high-resolution inelastic X-ray scattering (Baron *et al.*, 2000). Here, a very narrow bandwidth beam ($\Delta E/E \simeq 4 \times 10^{-8}$ at 22 keV) is focused onto the sample, with eight beam-defining apertures (in angle, energy and spatial extent) over the 100 m path to the sample position. Typically the final beam size is $\sim 60 \mu\text{m} \times 90 \mu\text{m}$ in FWHM, and the final aperture before the sample is $300 \mu\text{m} \times 300 \mu\text{m}$ or less. Meanwhile, scan times are 2–6 h, with experiments often requiring accumulation of data for as much as a day for a single spectrum. Thus stability is very important.

The main improvement from top-up operation at BL35XU was the stabilization of the power load on the high-heat-load Si(111) monochromator. As inelastic X-ray scattering experiments are flux-limited, this optic is operated at power loads up to 400 W, which leads to slow thermal drifts (\sim hours to days) that depend on the electron beam current. Even with the very long (150 h) lifetimes available previously in multi-bunch mode, there were noticeable drifts that had to be corrected, and more so for the several bunch modes (20–50 h lifetimes) that account for about half of the user operation. However, with top-up operation, and good running conditions, it is no longer necessary to adjust the high-heat-load monochromator, making beamline operation both easier and more efficient. This is illustrated in Fig. 22, which shows the flux measured just before the sample (after the final slit) for 7 d of operation with and without top-up operation. The improvement in stability, and intensity, of flux onto the sample is very clear.

Another benefit of top-up operation was the stabilization of the power load onto the high-resolution backscattering monochromator. The $\sim 100 \text{ mW}$ of power in the monochromatic beam is enough to locally heat a silicon crystal by a few tens of mK, creating a thermal gradient between the temperature sensor and the beam spot. This is power-load dependent and required correction before top-up operation began.

5. Conclusion

Top-up operation with good stability has been attained at SPring-8 by retrofitting of the accelerator complex. We have

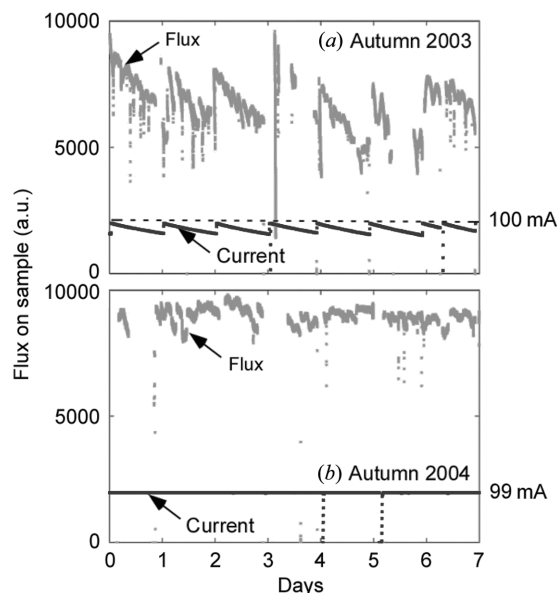


Figure 22 Flux on the sample and electron beam current at BL35XU at (a) conventional operation and (b) top-up operation. Similar experiments were in progress in both cases, with experienced users. Note that larger gaps in the grey trace are generally due to users opening the hutch to modify the sample set-up, while few-hour period oscillations are due to scan effects.

achieved a current stability of 10^{-3} , beam injection that is undetectable in any imaging experiment, purity of a level of 10^8 for isolated single bunches over the full user operation period, and a beam injection efficiency of 80–90% with the gaps of in-vacuum IDs fully closed. Experiments highlight the merits of top-up running for precise synchrotron radiation experiments. These include (i) $3 \times (1.5 \times)$ higher average photon flux for experiments using few (multi-) bunch modes, (ii) monitor-free operation in some cases, (iii) extremely high stability of the X-ray optics, and (iv) freely scheduled experiments.

Success of the top-up operation at SPring-8 was possible due to significant effort from all of the facility staff and visiting researchers. We would like to thank all the people who contributed to the realisation of the SPring-8 top-up operation. We also thank Assistant Professor Makoto Seto of Kyoto University for providing us with Fig. 18, and Mr Tetsuya Takagi of JASRI for providing the results of the radiation leakage measurements.

References

Ando, A., Amano, S., Hashimoto, S., Kinoshita, H., Miyamoto, S., Mochizuki, T., Niibe, M., Shoji, Y., Terasawa, M., Watanabe, T. & Kumagai, N. (1998). *J. Synchrotron Rad.* **5**, 342–344.
 Aoki, T., Fukami, K., Hosoda, N., Ohshima, T., Shoji, M., Tamura, K. & Yonehara, H. (2003). *Proceedings of the 20th Particle Accelerator Conference*, Portland, USA, pp. 2551–2553. Piscataway, NJ: IEEE.

Asaka, T., Hanaki, H., Hori, T., Kobayashi, T., Mizuno, A., Sakaki, H., Suzuki, S., Taniuchi, T., Yanagida, K., Yokomizo, H. & Yoshikawa, H. (2002). *Nucl. Instrum. Methods Phys. Res. A*, **488**, 26–41.
 Asaka, T., Kawashima, Y., Takashima, T., Kobayashi, T., Ohshima, T. & Hanaki, H. (2004). *Nucl. Instrum. Methods Phys. Res. A*, **516**, 249–269.
 Baron, A. Q. R., Tanaka, Y., Goto, S., Takeshita, K., Matsushita, T. & Ishikawa, T. (2000). *J. Phys. Chem. Solids*, **61**, 461–465.
 Böge, M. (2002). *Proceedings of the 8th European Particle Accelerator Conference*, Paris, France, pp. 39–43. Geneva: European Physical Society.
 Emery, L. (2001). *Proceedings of the 19th Particle Accelerator Conference*, Chicago, USA, pp. 2599–2601. Piscataway, NJ: IEEE.
 Emery, L. & Borland, M. (2002). *Proceedings of the 8th European Particle Accelerator Conference*, Paris, France, pp. 218–220. Geneva: European Physical Society.
 Fukami, K., Aoki, T., Hosoda, N., Nakatani, T., Ohshima, T., Takano, S., Tanaka, H., Yamashita, A. & Yonehara, H. (2004). *Proceedings of the 3rd Asian Particle Accelerator Conference*, Gyeongju, Korea, pp. 103–105. Pohang: Pohang Accelerator Laboratory.
 Hart, R., Benmore, C. J., Neufeind, J., Kohara, S., Tomberli, B. & Egelstaff, P. A. (2005). *Phys. Rev. Lett.* **94**, 047801.
 Hayakawa, S., Goto, S., Shoji, T., Yamada, E. & Gohshi, Y. (1998). *J. Synchrotron Rad.* **5**, 1114–1116.
 Ishiji, K., Yamasaki, H., Masui, T. & Hashizume, H. (2005). *J. Phys. Soc. Jpn.* **74**, 753–757.
 JAERI-RIKEN SPring-8 Project Team (1991). Conceptual Design Report, SPring-8 Project Part I Facility design [Revised]. SPring-8, Hyogo, Japan.
 Kawashima, Y., Asaka, T. & Takashima, T. (2001). *Phys. Rev. Special Topic AB*, **4**, 082001.
 Level, M. P., Brunelle, P., Chaput, R., Filhol, J. M., Herbeaux, C., Loulergue, A., Marcouillé, O., Marlats, J. L., Nadj, A., Tordeux, M. A., Chel, S. & Payet, J. (2002). *Proceedings of the 8th European Particle Accelerator Conference*, Paris, France, pp. 212–214. Geneva: European Physical Society.
 Liu, G. (2002). Personal communication.
 Loulergue, A., Tordeux, M. A., Daël, A., Corlier, M., Gros, P., Godefroy, J. M., Lebasque, P., Herbeaux, C., Marlats, J. L. & Denard, J. C. (2002). *Proceedings of the 8th European Particle Accelerator Conference*, Paris, France, pp. 593–595. Geneva: European Physical Society.
 Lüdeke, A. & Muñoz, M. (2002). *Proceedings of the 8th European Particle Accelerator Conference*, Paris, France, pp. 721–723. Geneva: European Physical Society.
 Maruyama, H. (2001). *J. Synchrotron Rad.* **8**, 125–128.
 Masaki, M. & Takano, S. (2003). *J. Synchrotron Rad.* **10**, 295–302.
 Nakamura, N. (2002). Personal communication.
 Nakamura, S. et al. (1990). *Proceedings of the 2nd European Particle Accelerator Conference*, Nice, France, pp. 472–474. Gif-sur-Yvette: Editions Frontières.
 Nakamura, T., Daté, S., Ohshima, T. & Kobayashi, K. (2004). *Proceedings of the 9th European Particle Accelerator Conference*, Lucerne, Switzerland, pp. 2649–2651. Geneva: European Physical Society.
 Nishino, Y., Kudo, T., Suzuki, M. & Ishikawa, T. (2003). *Proc. SPIE*, **5195**, 94–103.
 Ohkuma, H., Daté, S., Kumagai, N., Masaki, M., Nakamura, T., Ohshima, T., Soutome, K., Takano, S., Takao, M., Tamura, K. & Tanaka, H. (2003). *Proceedings of the 20th Particle Accelerator Conference*, Portland, USA, pp. 881–883. Piscataway, NJ: IEEE.
 Ohshima, T., Kumagai, N., Masaki, M., Matsui, S., Ohkuma, H., Soutome, K., Takao, M. & Tanaka, H. (2004). *Proceedings of the 9th European Particle Accelerator Conference*, Lucerne, Switzerland, pp. 414–416. Geneva: European Physical Society.
 Rivkin, L. et al. (1998). *Proceedings of the 6th European Particle Accelerator Conference*, Stockholm, Sweden, pp. 623–625. Bristol, UK: Institute of Physics Publishing.

- Scott, D. J., Clarke, J. A., Dykes, D. M., Holder, D. J., Jones, J. K., Kay, J., Marks, N., Owen, H. L., Poole, M. W., Smith, S. L., Suller, V. P., Varley, J. A. & Wyles, N. G. (2002). *Proceedings of the 8th European Particle Accelerator Conference*, Paris, France, pp. 617–619. Geneva: European Physical Society.
- Seto, M., Kitao, S., Kobayashi, Y., Haruki, R., Yoda, Y., Mitsui, T. & Ishikawa, T. (2003). *Phys. Rev. Lett.* **91**, 185505.
- Soutome, K., Liu, G., Kumagai, K., Kumagai, N., Ohkuma, H., Takao, M. & Tanaka, H. (1999). *Proceedings of the 18th Particle Accelerator Conference*, New York, USA, pp. 2337–2339. Piscataway, NJ: IEEE.
- Suzuki, H., Aoki, T., Ego, H., Hara, M., Hosoda, N., Kawashima, Y., Ohashi, Y., Ohshima, T., Tani, N., Yabashi, M. & Yonehara, H. (2000). *Nucl. Instrum. Methods Phys. Res. A*, **444**, 515–533.
- Suzuki, S., Asaka, T., Dewa, H., Hanaki, H., Kobayashi, T., Masuda, T., Mizuno, A., Taniuchi, T., Tomizawa, H. & Yanagida, K. (2004). *Proceedings of the 9th European Particle Accelerator Conference*, Lucerne, Switzerland, pp. 1327–1329. Geneva: European Physical Society.
- Suzuki, Y., Takeuchi, A., Takano, H., Ohigashi, T. & Takenaka, H. (2001). *Jpn. J. Appl. Phys.* **40**, 1508–1510.
- Takao, M., Ohshima, T., Sasaki, S., Schimizu, J., Soutome, K. & Tanaka, H. (2004). *Proceedings of the 9th European Particle Accelerator Conference*, Lucerne, Switzerland, pp. 417–419. Geneva: European Physical Society.
- Tamura, K. & Aoki, T. (2004). *Proceedings of the 1st Annual Meeting of Particle Accelerator Society of Japan*, Funabashi, Japan, pp. 581–583. Funabashi, Chiba: Nihon University.
- Tanaka, H., Aoki, T. *et al.* (2004). *Proceedings of the 9th European Particle Accelerator Conference*, Lucerne, Switzerland, pp. 222–224. Geneva: European Physical Society.
- Tanaka, H., Kumagai, K., Kumagai, N., Masaki, M., Ohkuma, H., Soutome, K. & Takao, M. (2000). *Proceedings of the 7th European Particle Accelerator Conference*, Vienna, Austria, pp. 1575–1577. Geneva: European Physical Society.
- Tanaka, H., Ohshima, T., Soutome, K. & Takao, M. (2005). *Nucl. Instrum. Methods Phys. Res. A*, **539**, 547–557.
- Tanaka, H., Ohshima, T., Soutome, K., Takao, M. & Takebe, H. (2004). *Proceedings of the 9th European Particle Accelerator Conference*, Lucerne, Switzerland, pp. 1330–1332. Geneva: European Physical Society.
- Tanaka, H., Soutome, K., Takao, M., Masaki, M., Ohkuma, H., Kumagai, N. & Schimizu, J. (2002). *Nucl. Instrum. Methods Phys. Res. A*, **486**, 521–538.
- Tanaka, H., Soutome, K., Takao, M. & Schimizu, J. (2001). *Proceedings of the 13th Symposium on Accelerator Science and Technology*, Suita, Japan, pp. 83–85. Osaka: Osaka University.
- Tsumaki, K., Shimada, K., Kajimoto, T., Yonehara, H. & Kumagai, N. (2004). *IEEE Trans. Appl. Superconduct.* **14**, 433–436.
- Ueng, T. S., Hsu, K. T., Chen, J., Lin, K. K. & Weng, W. T. (1996). *Proceedings of the 5th European Particle Accelerator Conference*, Sitges, Spain, pp. 2477–2479. London: Taylor and Francis.
- Yabashi, M., Tamasaku, K. & Ishikawa, T. (2001). *Phys. Rev. Lett.* **87**, 140801.
- Yanagida, K., Asaka, T., Dewa, H., Hanaki, H., Kobayashi, T., Mizuno, A., Suzuki, S., Taniuchi, T. & Tomizawa, H. (2004). *Proceedings of the 22nd International Linear Accelerator Conference*, Lübeck, Germany, pp. 464–466. Hamburg: Deutsches Elektronen-Synchrotron (DESY).
- Yoshioka, M., Ohshima, T., Sasaki, S. & Ohata, T. (2003). *Proceedings of the 14th Symposium on Accelerator Science and Technology*, Tsukuba, Japan, pp. 428–430. Tsukuba: High Energy Accelerator Research Organization (KEK).